Journal of *Marine Science and Engineering*

MDPI

Article

Using Forward and Backward Particle Tracking Approaches to Analyze Impacts of a Water Intake on Ichthyoplankton Mortality in the Appomattox River

Qubin Qin [1], Jian Shen [1,*], Troy D. Tuckey [1], Xun Cai [1,2] and Jilian Xiong [1,3]

[1] Virginia Institute of Marine Science, William & Mary, Gloucester Point, VA 23062, USA
[2] ORISE Research Participation Program at EPA, Chesapeake Bay Program Office, Annapolis, MD 21401, USA
[3] School of Oceanography, University of Washington, Seattle, WA 98195, USA
* Correspondence: shen@vims.edu

Abstract: Municipal intakes of surface water have various uses, and their impacts on the aquatic environment and ecosystem, such as the impingement and entrainment of ichthyoplankton, are a major concern. A robust assessment of the intake impacts on ichthyoplankton in a system generally requires modeling efforts that can simulate the transport and dispersal pathways of the ichthyoplankton. However, it is challenging to simulate hydrodynamics with a high-resolution grid at the scale needed for intake screen sizes in a large system. In this study, a 3D unstructured grid model with a fine resolution grid (<1 m) was developed to investigate potential impacts of an intake on aquatic resources in a tidal freshwater estuary. This approach enables us to directly estimate intake-induced mortality. With the use of the coupled particle-tracking model, we evaluated the total and maximum daily removal rates of particles by the intake that can be used to estimate percent mortality of ichthyoplankton. We further investigated how impacts from the intake vary with spawning locations, flow conditions, and vertical migration velocity of ichthyoplankton. A risk assessment was conducted based on designed flow of water withdrawals. This approach is widely applicable and can address impacts of water intakes in other systems.

Keywords: water intake; fish; ichthyoplankton; egg; larvae; particle tracking; environment; model

Citation: Qin, Q.; Shen, J.; Tuckey, T.D.; Cai, X.; Xiong, J. Using Forward and Backward Particle Tracking Approaches to Analyze Impacts of a Water Intake on Ichthyoplankton Mortality in the Appomattox River. *J. Mar. Sci. Eng.* **2022**, *10*, 1299. https://doi.org/10.3390/jmse10091299

Academic Editor: Francesco Tiralongo

Received: 8 July 2022
Accepted: 12 September 2022
Published: 14 September 2022

1. Introduction

Surface water intakes have increased in many coastal and estuarine systems for various uses, such as supply of drinking water, irrigation for agriculture, providing cooling water for power plants, desalination for potable water sources, as well as for other industrial applications. The construction and operation of surface water intake systems can have adverse impacts on aquatic resources since many intake systems are located in highly productive estuaries and coasts that contain critical spawning and nursery habitats. One of the key potential ecosystem impacts is increased mortality of aquatic organisms, especially those in early life stages, such as fish eggs and larvae [1–3]. Mortality of aquatic fauna can occur from the operation of a surface water intake by entrainment (passage of life history stages through the screen that is smaller than the screen slots), impingement (trapping of life history stages against the screen that is larger than the screen slots), and blunt contact (causing unrecoverable bodily harm to fragile eggs and larvae). In many countries, including the US, Europe, and Australia, environmental impacts of proposed intake systems are required before permits are issued for construction and operation [3]. Different modeling approaches have been developed since the 1970s to assess potential impacts of intake operations on fish populations, such as adult equivalent loss, fecundity hindcasting, and empirical transport models [1–5]. Meanwhile, there is a debate about whether an intake will lead to significant loss of fish as a result of impingement and entrainment [3,6]; evidence shows clearly that ichthyoplankton are more vulnerable than adults (e.g., Ref. [7]), and even those larvae with

relatively strong swimming abilities cannot avoid entrainment when the intake velocity through the screen is fast [8]. Thus, it is critical to estimate the loss of ichthyoplankton caused by intake operations to support effective management of aquatic resources.

The dispersal of ichthyoplankton has been recognized as a critical factor in determining potential impacts of surface water intakes [9,10]. The dispersal or transport of ichthyoplankton in aquatic systems determines their distribution and probability of encounter with intakes, and it is assumed that higher encounter probability results in higher mortality due to impingement, entrainment, and blunt contact with intake screens (referred to as conditional mortality rate hereafter). Quantifying the magnitude of mortality caused by surface water intakes is the main objective so that potential impacts on aquatic resources can be properly assessed. Because of the complex aquatic environment where ichthyoplankton are found, dispersal pathways should be identified using a numerical model that can simulate both the hydrodynamics of a particular system and the transport and behavior of ichthyoplankton in the system. Since intake screens occupy a vertical position in the water column, a 3D model is needed to properly simulate ichthyoplankton transport, swimming behavior, and interaction with intakes. Unfortunately, there are limited modeling studies that include a coupled hydrodynamic model with a particle tracking model that also captures the vertical migration capability of fish [9–11]. While these studies explicitly simulated hydrodynamics in the systems they investigated, they were unable to provide accurate simulations of currents near the intakes due to coarse model grids. The size of intakes is usually small (at the scale of meters) compared with the larger-scale (10 s–100 s km) aquatic system where they are placed. To accurately represent flows near an intake, a high-resolution grid at the scale of the intake screen or less is needed.

An additional consideration in assessing potential impacts of surface water intakes involves fish spawning locations relative to intake structures. Fish spawn at different locations in aquatic systems, and the resulting ichthyoplankton may experience different transport conditions depending on where they originate. It can be expected that ichthyoplankton originating at one location may be more vulnerable to the intake than if they originate at another location [11]. Thus, it is important to assess the influence of spawning location while considering potential impacts of surface water intakes on ichthyoplankton survival.

In estuaries, tidal currents and river discharge are two major forces that contribute to the hydrodynamics on short- and long-term timescales. While tides change magnitude over a spring–neap cycle, the impact of river discharge on hydrodynamics changes on longer timescales, such as seasonally and interannually. It is important to investigate how changes in flow conditions, especially due to river discharge, alter the transport of ichthyoplankton and, hence, potential impacts of surface water intakes [7,10]. For example, it has been suggested that higher river flow results in less time for larvae and eggs to stay in the vicinity of the intake and, therefore, leads to lower probability of entrainment [9].

In addition to spawning location, tidal currents, flow, egg density, and larval fish behavior can have an impact on their distribution in the water column and the potential to interact with surface water intakes. Ichthyoplankton have the ability to change their vertical position in the water column through buoyancy (as a result of the density of eggs relative to the density of the surrounding water) or swimming behaviors (larvae), which can significantly affect the dispersal and distribution of ichthyoplankton in estuaries [12]. Thus, the impacts of surface water intakes are expected to change with different vertical velocities of ichthyoplankton particles. Previous modeling studies using particle tracking models, however, usually assume neutrally buoyant, passive particles and rarely consider active particles with vertical velocities [9–11].

To address the influence of the issues described above, we investigated the potential impacts of a typical municipal surface water intake on ichthyoplankton survival in the tidal portion of the Appomattox River, Virginia. We developed a fine-resolution 3D numerical model to simulate the hydrodynamics of the system and included a particle tracking model that includes active and passive particles to simulate potential ichthyoplankton behaviors and effects on transport processes. The intake screens were resolved in the model grid

to a resolution of less than 1 m in the vicinity of the intake structure. Thus, changes in hydrodynamic conditions due to the construction and operation of the intake can be evaluated at scales relevant to ichthyoplankton survival. We used a particle tracking model to simulate fish egg and larval movement to evaluate probabilistic increases in assumed mortality due to operation of the intake. We further investigated how the impacts of the intake vary with different spawning locations, flow conditions, and vertical velocities of ichthyoplankton that are specific to this system, which provides an understanding of potential impacts of intake operations on ichthyoplankton survival.

2. Methods

2.1. Study Area

The Appomattox River is a tidal-freshwater tributary of the James River, VA, USA (Figure 1a). The water temperature varies from below 5 °C in winter to above 30 °C in summer, and the salinity is less than 0.5 psu, with a tidal range of about 0.75 m. In the Upper James River and its tributaries, including the Appomattox River, river discharge and tide play important roles in regulating the physical transport processes, while wind has less of an influence on dynamics [13].

We obtained time series data of river discharge for the Appomattox River from a local USGS station (https://waterdata.usgs.gov/monitoring-location/02041650/ (accessed on 17 February 2019)) for the period from 1 October 1969 to 16 February 2019. The mean and median flows were 35.7 and 17.7 m^3 s^{-1}, respectively (Figure 2a), and the 10th and 90th percentiles were 3.6 and 85.2 m^3 s^{-1}, respectively.

2.2. Ichthyoplankton in the Study Area

We are not aware of any ichthyoplankton data from the Appomattox River and, thus, used data from a long-term seine survey conducted in the nearby James River to identify species that may be susceptible to surface water intakes. Fish community data were obtained from the VIMS Striped Bass Seine Survey (seine survey hereafter) and were used to characterize fish species in the James River [14]. The seine survey has been conducted since 1965, although the time series for this analysis was restricted to more recent years as abundance of fish in Chesapeake Bay river systems have changed over time (e.g., decline in American shad). The seine survey is conducted during summer and provides data on the juvenile life stage of resident species, as well as others that use these habitats seasonally as nurseries for larvae and juveniles. We used the most recent 20 years of seine survey data (1999–2018) to determine a subset of species that spawn within Virginia's river estuaries, are important components of the local ecosystem, and may be vulnerable to the intake. The representative fish species we chose are blueback herring (*Alosa aestivalis*), which spawn from April to May and have semi-demersal eggs [15], inland silversides (*Menidia beryllina*), which spawn from April to September and have demersal and sticky eggs [16,17], and striped bass (*Morone saxatilis*), which spawn from April to June and have buoyant eggs [18]. Blueback herring spawn in a variety of habitats, with most spawning occurring in the main portion of tidal freshwater areas, where striped bass spawning also occurs [15,19]. Inland silversides spawn along the shoreline, where eggs form stick mats in the shallow waters [16]. These species were selected to represent a range of biological characteristics that the tidal freshwater ichthyofauna possess. These species are common to all tidal rivers in Virginia and have published details about their life history that can be used in the modeling exercise. They represent managed species (striped bass, blueback herring) and forage species (inland silversides) that would be vulnerable to the intake and thus relevant to the discussion of potential impacts.

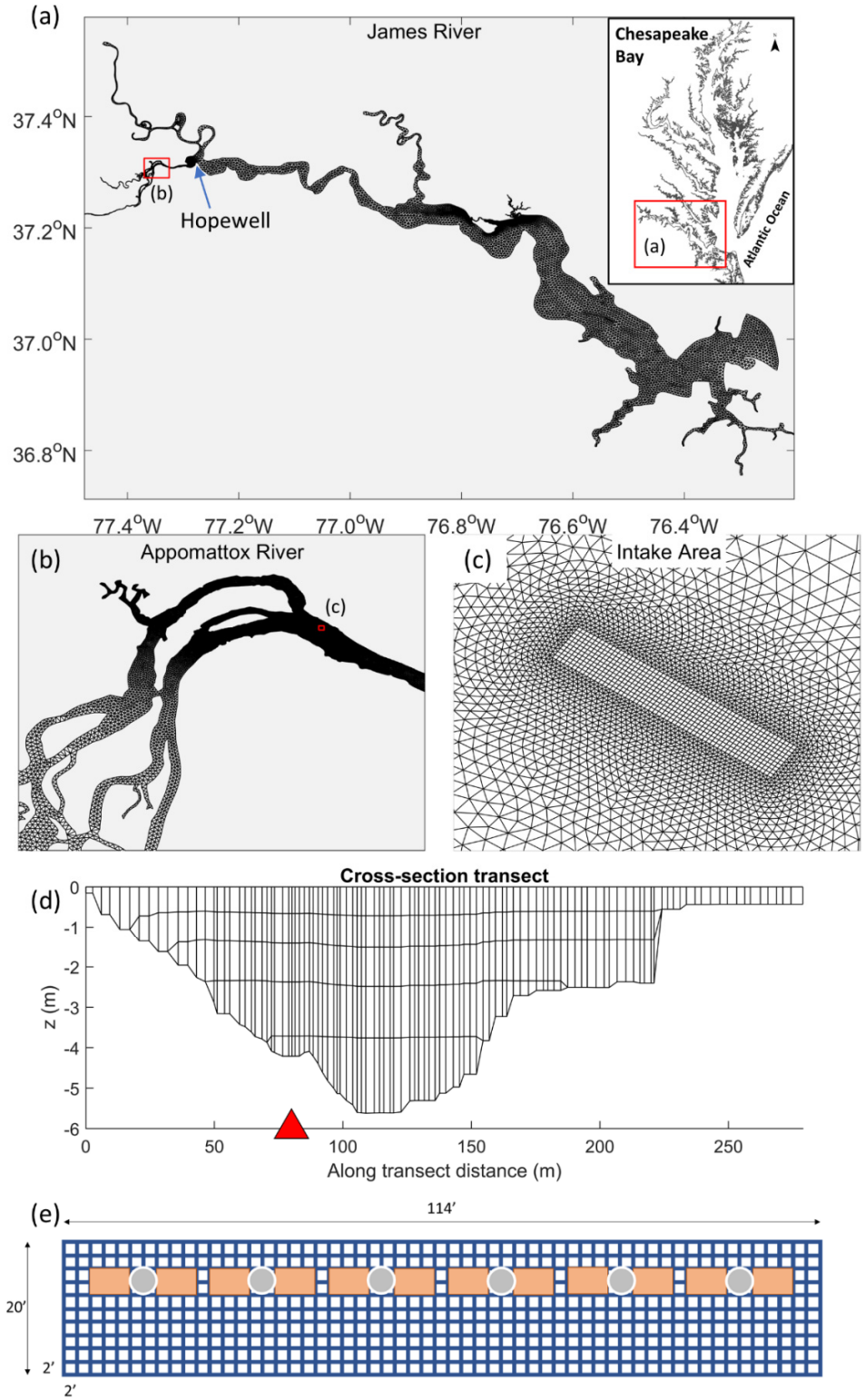

Figure 1. The extended James River model grid with high resolution near the vicinity of the intake. (**a**) The horizontal grid for the James River. (**b**) The refined horizontal grid for the Appomattox River. (**c**) The grid of high resolution for the intake area. (**d**) A cross-sectional transect showing the vertical layers (not the vertical grid) at the intake area (looking downstream). The red triangle marks the location of the intake. (**e**) The horizontal grid designed for the intake area. The length is 34.7 m (114 feet), and the width is 6.1 m (20 feet). Each of the six functional intake screens is represented by 16 grid elements, and the size of each element is 0.61 m × 0.61 m.

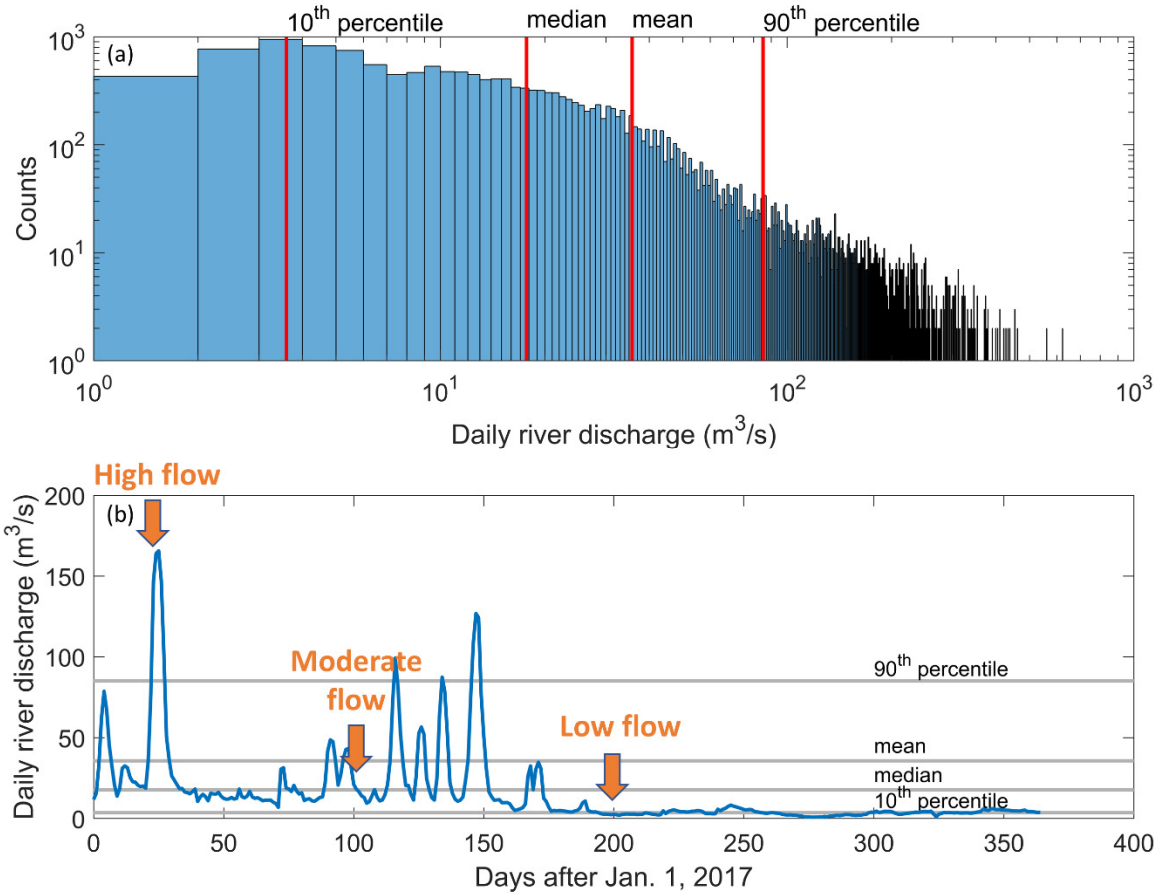

Figure 2. (**a**) Statistics of daily river discharge of the Appomattox River from 1969 to 2019. (**b**) Daily river discharge of the Appomattox River in 2017, the year used for hydrodynamic simulations. Arrows mark the selected dates for scenarios 8–13 to investigate the impacts of river flow conditions.

2.3. Model Development and Hydrodynamic Scenarios

The Chesapeake Bay Semi-implicit Cross-scale Hydroscience Integrated System Model (SCHISM) that has been calibrated and used in different applications [20–22] was modified to develop the model for the Appomattox River and the adjacent James River. The model grid was refined in the tidal Appomattox and the upper tidal James Rivers to accurately represent the complex geometry and bathymetry in the tidal freshwater region (Figure 1a–c). SCHISM uses a semi-implicit time-stepping scheme applied in a hybrid finite-element and finite-volume framework to solve Navier–Stokes equations and uses a Eulerian–Lagrangian method to treat the momentum advection [23]. The unstructured grid model is flexible and is capable of simulating complex changes in geometry within 1–10 m resolution. In the vertical dimension, the model uses a highly flexible and efficient hybrid coordinate system [24]. The vertical model grid over a cross-section at the intake is shown in Figure 1d.

The horizontal model grid has a total of 54,218 grid elements. The intake area is represented by 570 quadrilateral grid elements, with a resolution of about 0.61 m, and each intake screen is represented by 16 grid elements (96 elements in total for the six intake screens; Figure 1e). The water depth is set to be 3.78 m mean low water (MLW) at the intake area, and the water column is resolved by five vertical layers. The bathymetry data for the Appomattox River were obtained from a National Oceanic and Atmospheric Administration chart (NOAA Chart #12252), and those for the area around the intake were provided by Waterway Surveys & Engineering, Ltd. With this high-resolution model grid, the model can simulate complex dynamics in the near-field of the intake. In the present study, it is assumed that water is withdrawn continuously by the intake, and the

withdrawal rate was 40 mgd (i.e., 1.7525 m^3/s). The withdrawal rate for each grid element representing the intake is 0.01826 $m^3\ s^{-1}$ (i.e., 1.7525 $m^3\ s^{-1}$ divided by 96).

The hydrodynamic model was first run For one year (2017) only to provide the hydrodynamic fields that inform the particle tracking model. Two cases, one without the intake (referred to as "Normal") and one with the intake (referred to as "Withdrawal"), were conducted to evaluate the changes to the hydrodynamics in the Appomattox and James Rivers due to construction of the intake.

2.4. Particle Tracking Model

The particle tracking model (PTM) has been broadly applied to coastal projects, including studies of dredged material dispersion and fate, and oyster and larval fish dispersion and recruitment (e.g., Refs. [9,25,26]). The particle tracking algorithms can incorporate transport, settling, deposition, mixing, and resuspension processes. In this study, we used a particle tracking model coupled with the SCHISM modeling system (schism.wiki) to simulate fish egg and larval transport. The PTM is a Lagrangian particle tracker designed to allow the user to simulate particle transport processes [27–29]. Each particle can represent an individual or a cluster of ichthyoplankton. Different densities and mortality rates of fish eggs and larvae of different species can be added to the model to simulate diverse physical and biological behaviors. Although the actual densities of eggs/larvae vary with time, we can estimate losses as a proportion of organisms in the river that encounter the intake and do not need absolute numbers. With the combination of the high-resolution hydrodynamic model and the PTM, the complex and dynamic fields with high swirl and vortices near the intake can be accurately simulated. Therefore, the removal of fish eggs and larvae can be simulated directly in our study with the use of the fine-resolution grid. So long as particles encounter the intake, they are removed from the system. This avoids uncertainty introduced by the probability method to determine entrainment that is used by some models with coarse-resolution grid [4,9]. The computed removal rate of particles provides an estimate of the conditional mortality rate resulting from the operation of the intake.

2.5. Particles That Represent Ichthyoplankton

It is well known that larval fish swimming behavior can alter the distribution of the larvae in aquatic systems. To better represent fish eggs or larvae, two different particles were used in the study—passive particles vs. active particles. The passive particles are neutrally buoyant particles, such as neutrally buoyant fish eggs or larvae. Their transport is strictly determined by the hydrodynamic field. The active particles are allowed to move upward or downward in the model to represent the rise of buoyant eggs or settling of heavier demersal eggs in the water column, as well as the upward swimming behaviors of fish larvae.

The vertical speeds of fish eggs (ω) are dependent on the buoyancy and gravity of the particles, which is computed using the Stokes equation:

$$\omega = \frac{(\rho_e - \rho_w)}{18\mu} g R^2$$

where g is the gravitational field strength (m s^{-2}), R is the diameter of the spherical particle (m), ρ_e is the mass density of the egg (kg m^{-3}), ρ_w is the mass density of water (kg m^{-3}), and μ is the dynamic viscosity (kg $(m{\cdot}s)^{-1}$), μ = 0.001 kg $(m{\cdot}s)^{-1}$ at 20 °C. The velocity computed using Stokes equation is usually applied for particles with a Reynold's number ($Re_p = \rho_w \frac{\omega R}{\mu}$) less than 0.5 [30]. Outside of this range, turbulent drag due to the wake behind the particle becomes important and leads to smaller vertical speed of the particles than that computed using the Stokes equation.

The mass density of fish eggs varies with species and environmental conditions, such as temperature. However, the effect of water temperature on egg velocity through the change in mass density of eggs is considered to be negligibly small [31]. The eggs of striped bass in the Pamunkey River, a tidal freshwater river in Chesapeake Bay, have a mass density

of around 1.0018 g cm^{-3} and a diameter of 1.84 mm [32]. In our study area, where salinity is less than 0.5 psu, the mass density of water is about 1.0 g cm^{-3}; thus, egg density is greater than the density of water, $\rho_P > \rho_w$, and the eggs can be considered demersal eggs [31]. This provides a settling velocity, v = 0.0033 m s^{-1} (or 0.33 cm s^{-1}), and provides a base velocity for fish eggs in the study area. The egg diameter of inland silversides is between 0.9–1.2 mm [16] and 0.87–1.11 mm for the blueback herring [33]. However, using these values in Stokes equation results in an egg velocity of ω = 0.0033 cm s^{-1}, which equates to a Reynold's number of Re_p = 6.1, beyond the allowable range for using the Stokes equation ($Re_p < 0.5$). Thus, the computation of vertical speed for eggs used other empirical formulae based on experiments [30,34]. Here, we used the formula for a spherical particle found in Ref. [35]: $\omega = \frac{SgR^2}{18v+(0.3SgR^3)^{0.5}}$, where $S = (\rho_e - \rho_w)/\rho_w$ and $v = \mu/\rho_w$ is the kinematic viscosity of water (10^{-6} kg (m·s)$^{-1}$ at 20 °C). Using this equation, the settling velocity for fish eggs in the study area is about 0.25 cm s^{-1}, a little less than 0.33 cm s^{-1} obtained from the Stokes equation. Using other empirical equations resulted in similar velocities.

The settling velocity of eggs in natural systems can be significantly different from the speeds computed using equations that are based on laboratory experiments [30]. In estuaries where turbulent mixing is significant, settling velocities can vary widely. For example, the settling velocity of particles in turbulent flows can either increase or decrease compared to that in laminar flows [36]. As a result, to broaden the applicability of the model, we considered the settling velocities of eggs that span a wide range in nature and chose five representative vertical velocities (−1, −0.3, −0.1, −0.01, and −0.001 cm s^{-1}) (Table 1). By using a range of vertical velocities, we account for the variability in egg diameter and egg density that exists among fish species and represent the suite of fish that may be spawning in the vicinity of the intake rather than a single species. Note that the smallest velocity of −0.001 cm s^{-1} (about −0.86 m d^{-1}) is close to the values used in numerical models for the settling velocity of phytoplankton in estuaries [37].

In developing the model to include larval fish behavior, we assumed a constant upward swimming velocity for each active particle. Downie et al. [38] argue that routine swimming speeds or the in situ swimming speeds of fish larvae should be used in the model. Since we do not know the actual swimming speed for many species, we chose a range of possible swimming speeds. For example, the swimming speed of striped bass larvae is between 0.54 cm s^{-1} and 2.64 cm s^{-1} [39]. Other species are likely to have faster and slower speeds compared with striped bass, and swimming speed also depends on fish length. Thus, by using two different rates in the model, we account for a wide range of potential swimming speeds that may be observed. We ignored the horizontal swimming speed of larvae since it is negligible compared to the horizontal advections dominated by currents. In total, we tested seven vertical velocities to represent different groups of eggs (buoyant, neutrally buoyant, and demersal) and larvae (Table 1). We believe the seven vertical velocities used in this study represent a variety of potential sinking/swimming velocities representative of eggs and larvae found in the Appomattox River.

Table 1. Particle types, vertical velocity, and the life stage they represent. Negative values indicate downward velocities.

Particle	Vertical Velocity (cm s^{-1})	Life Stage
Passive	0	Neutrally buoyant eggs
Active	−1	Demersal eggs
Active	−0.3	Demersal eggs
Active	−0.1	Demersal eggs
Active	−0.01	Demersal eggs
Active	−0.001	Demersal eggs
Active	1	Larvae
Active	10	Larvae

2.6. Forward and Backward Particle Tracking Approaches

Both forward and backward particle tracking methods were used as each method provides a different perspective on the interaction between particles and the intake. For the forward tracking method, we chose the locations to release the particles and tracked their trajectories at each time point during the study period ($t = t_0, t_1, \ldots, t_{end-1}, t_{end}$). The forward tracking method directly computes the percentage of particles that ultimately encounter the intake, which is the total percent removed. The maximum daily removal rate is further computed by counting the highest daily percent over the study period. For the backward tracking method, given a simulation period, the particles are released at the end of the period ($t = t_{end}$) within the model grid cells representing the intake, and the velocities are reversed in their directions and we track the movement of the particles backward to the beginning of the period ($t = t_{end}, t_{end-1}, \ldots, t_1, t_0$). The backward tracking method provides information on the origins of particles that encounter the intake.

Understanding the potential influence of a particular grid cell on the number of particles that are removed by the intake can be based on time or the number of particles that originate from that grid cell. The overall frequency of particles (or eggs and larvae) that are removed by the intake from one specific grid cell is defined as the ratio of the points in time that particles from that grid cell are removed by the intake divided by the total number of time points that exist during the chosen time period. Denote $f_{i,j}$, the frequency at the grid cell j at time point $t = t_i$; if there is more than one particle in that grid cell that is removed by the intake, the frequency equals 1 ($f_{i,j}$ = 1) at that time point; otherwise, $f_{i,j}$ equals 0. The overall frequency of each grid cell over the computation period was computed as $\langle f_j \rangle = \frac{1}{N} \sum_i f_{i,j}$, where N is the total number of time points during the simulation period. For example, if the total simulation period is 1 day, and time is assessed every 1 h, then N = 1 day/1 h = 24 h/1 h = 24. If the frequency of a grid cell equals one, then that means that this grid cell always has a fraction of particles that are removed by the intake during the simulation period (e.g., in the example provided, the frequency would be 24 time periods that the grid cell contained a particle that was removed by the intake divided by 24 h that the simulation was run, 24/24 = 1). If the grid cell is located at the head of the estuary, it suggests how frequently particles released from the freshwater flow are removed by the intake. Note that, for short run periods, the frequency only represents the frequency of particles at that location that are removed by the intake during that period (i.e., the frequency is dependent on the time period that was chosen and not representative of longer time periods). Thus, for areas that are relatively far from the intake, the computed frequency does not represent their long-term means. By examining the frequency distribution, the impact area can be evaluated.

The other method, based on counts of particles, that was used to assess the impact of individual grid cells is called: *Contribution*. The source of particles (or larvae or eggs) from each grid cell was evaluated by estimating the percentage of particles coming from that grid cell that are removed by the intake during the simulation period. For each time point t_i, $m_{i,j}$ denotes the number of particles in grid cell j that ultimately encounter the intake. In the back-tracking model, $m_{i,j}$ is computed by counting the number of particles in that grid cell at t_i. The contribution of one grid cell j over a portion of the computation period (from the beginning of the back tracking t_{end} to the time point t_i) was computed as $Contribution_{i,j} = \frac{1}{M_i} m_{i,j}$, where $M_i = \sum_j m_{i,j}$ is the total number of particles in the study area at t_i. Thus, the contribution of grid cell j over the entire computation period (from t_{end} to t_0) was computed as $Contribution_{0,j} = \frac{1}{M_0} m_{0,j}$.

2.7. Model Scenarios

2.7.1. Forward Tracking Scenario

Multiple forward particle tracking scenarios were conducted to investigate the potential impacts of the intake on ichthyoplankton survival (Table 2). We first designed seven forward tracking scenarios (scenarios 1–7) using around 10,000 passive particles to

evaluate the impacts of release method (one-time release of all particles at a given time vs. continuous release of particles over a period of time) and location on the percentage of particles that encounter the intake (Figures 3 and S1). By testing different release locations and release methods, we are able to evaluate which method and location leads to the greatest removal of particles due to the intake. To evaluate any potential bias resulting from the initial number of particles (10,000) that were released, we repeated selected scenarios that had non-zero removal of particles by the intake (scenarios 1–3, and 6) with a ten-fold increase in particle number (i.e., 100,000 particles). The results show that the percent of particles removed by the intake in the 10-fold scenarios are nearly identical to those from the original scenarios 1–3 and 6 (Table S1), and the performed Wilcoxon signed rank test shows that there is no statistically significant difference in the median of the daily removal rate between each pair of scenarios. Thus, 10,000 particles are sufficient to provide an accurate estimate of potential impacts for this study. For one-time scenarios, the release region is designed at the scale of kilometers, which is on the scale of tidal excursion [40]. For scenarios 6 and 7, particles were released continuously over a period of 21 days (5 January–11 April 2017), and the number of the particles released each day was proportional to the freshwater discharge of the river (Figure S2). This assumes that the loadings of fish eggs or larvae are proportional to freshwater discharge. Thus, these two scenarios account for eggs or larvae transported by river discharge from upstream locations that are beyond the model domain. Moreover, these seven scenarios show the movement of particles under moderate flow conditions. In scenarios 1–5, released on 11 April 2017, particles experience an average discharge of 26.5 m^3 s^{-1} during the release date and one day before (10 April and 11 April); for scenarios 6–7, the 21-day release occurs during an average discharge of 28.7 m^3 s^{-1}. These two discharge rates are between the median discharge of 17.7 m^3 s^{-1} and the mean discharge of 35.7 m^3 s^{-1} over the 50-year time-series (Figure 2).

Scenarios 8–13 were conducted to investigate the effects of flow on the percent of particles that encounter the intake. On timescales longer than the spring–neap tide cycle, the change in flow conditions is largely determined by variability in river discharge. Thus, the scenarios were designed to account for different river discharge rates. For high-flow, one-time release scenarios, particles were released on 24 January 2017 at a discharge rate of 112.3 m^3 s^{-1} (average discharge from 23 January and 24 January), which was higher than the 90th percentile from the discharge time series (Figure 2). The mean discharge for the next five days reached 145.1 m^3 s^{-1}, exceeding the 95th percentile of the discharge rate for the time series. For low-flow, one-time release scenarios, particles were released on 20 July 2017 at an average discharge rate of 2.5 m^3 s^{-1} (average of discharge rates from 19 July and 20 July), which was lower than the 10th percentile of the time series (Figure 2). The mean discharge for next five days was 2.4 m^3 s^{-1}. For the high-flow, continuous release scenarios, particles were released continuously beginning on 24 January 2017 (Figure S3), at a 21-day-average discharge of 50.3 m^3 s^{-1} (83th percentile). For the low-flow, continuous release scenarios, particles were released continuously beginning on 20 July 2017 (Figure S4), at a 21-day-average discharge of 2.78 m^3 s^{-1} (below 10th percentile). Note that, because we focused on the transport processes and not biological processes, the study period does not necessarily coincide with the spawning periods of the species. We chose the three periods in 2017 to investigate impacts of the intake under different flow conditions. The different spawning periods are also likely to experience different flow conditions, such as shifts between the wet and dry years, so the model results should be applicable across species and flow conditions.

In addition, 14 one-time release scenarios (scenarios 14–27) and seven continuous release scenarios (scenarios 28–34) were conducted for each vertical velocity of the active particles. Because it is more meaningful to assess worst-case situations for the intake-caused mortality of eggs or larvae, we focused on low flow conditions that potentially result in high conditional mortality rates.

For this study, we only released particles at the surface for all the forward tracking scenarios and did not explore the results if the particles were released at different vertical

positions in the water column. We expect that any differences due to the vertical position of particle releases would be small because of the shallow water depth and strong vertical mixing found in this tidal freshwater estuary. All scenarios were tracked for 30 days after the release of particles. Moreover, the non-parametric Kruskal–Wallis test was performed to statistically compare the results of the forward tracking scenarios.

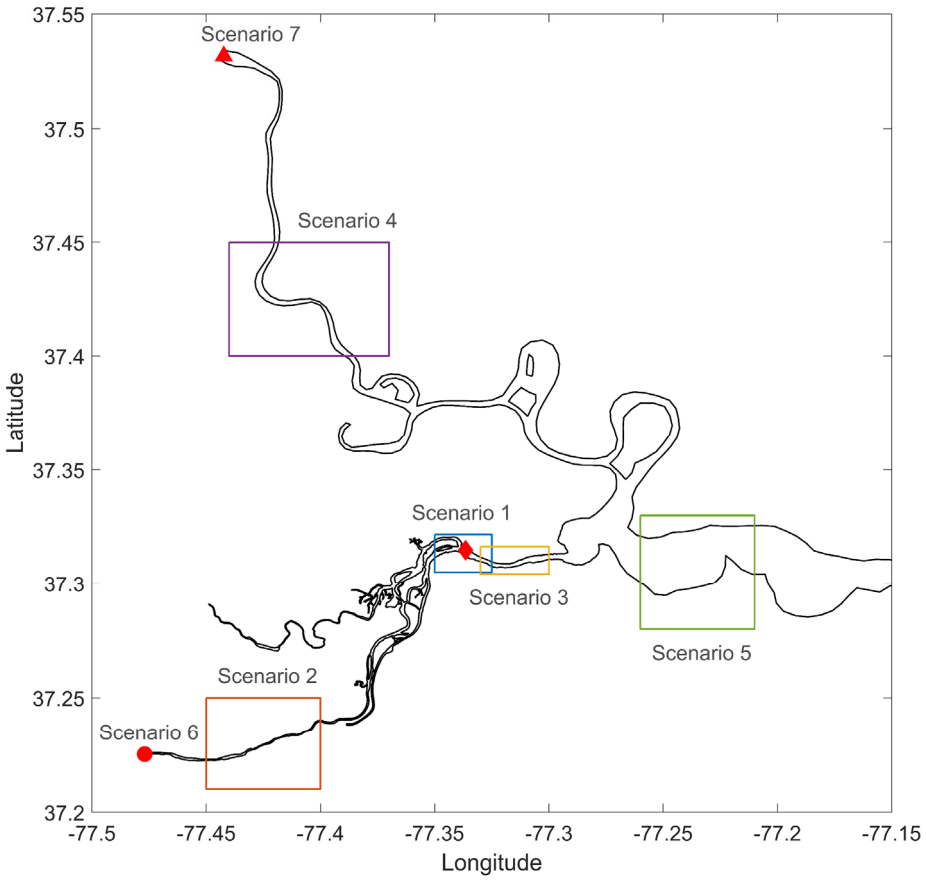

Figure 3. Map showing the release locations of particles for the seven scenarios of the forward particle tracking model (scenarios 1–7). The red diamond shows the location of the intake.

Table 2. The release method, location, flow condition, and vertical velocity of the 34 forward particle tracking scenarios. In those scenarios where particles are released continuously, the release period is 21 days, and the number of particles released is proportional to daily freshwater discharge. The vertical velocity of the particle can be either upward (+) or downward (−).

Scenario	Release Method	Release Location	Flow Condition	Vertical Velocity (cm s^{-1})
1	One time	Vicinity of the intake in the Appomattox	Moderate	0
2	One time	Upstream of the intake in the Appomattox	Moderate	0
3	One time	Downstream of the intake in the Appomattox	Moderate	0
4	One time	Above Hopewell in the James	Moderate	0
5	One time	Below Hopewell in the James	Moderate	0
6	Continuously	Head of the Appomattox of the model grid	Moderate	0
7	Continuously	Head of the James of the model grid	Moderate	0

Table 2. *Cont.*

Scenario	Release Method	Release Location	Flow Condition	Vertical Velocity (cm s^{-1})
8	One time	same as Scenario 1	High	0
9	One time	same as Scenario 1	Low	0
10	One time	same as Scenario 2	High	0
11	One time	same as Scenario 2	Low	0
12	Continuously	same as Scenario 6	High	0
13	Continuously	same as Scenario 6	Low	0
14	One time	same as Scenario 1	Low	−1
15	One time	same as Scenario 1	Low	−0.3
16	One time	same as Scenario 1	Low	−0.1
17	One time	same as Scenario 1	Low	−0.01
18	One time	same as Scenario 1	Low	−0.001
19	One time	same as Scenario 1	Low	1
20	One time	same as Scenario 1	Low	10
21	One time	same as Scenario 2	Low	−1
22	One time	same as Scenario 2	Low	−0.3
23	One time	same as Scenario 2	Low	−0.1
24	One time	same as Scenario 2	Low	−0.01
25	One time	same as Scenario 2	Low	−0.001
26	One time	same as Scenario 2	Low	1
27	One time	same as Scenario 2	Low	10
28	Continuously	same as Scenario 6	Low	−1
29	Continuously	same as Scenario 6	Low	−0.3
30	Continuously	same as Scenario 6	Low	−0.1
31	Continuously	same as Scenario 6	Low	−0.01
32	Continuously	same as Scenario 6	Low	−0.001
33	Continuously	same as Scenario 6	Low	1
34	Continuously	same as Scenario 6	Low	10

2.7.2. Backward Tracking Scenario

Whereas the forward tracking scenarios are straightforward in how to estimate the percentage of particles that are removed by the intake for given release locations, the number of release locations is limited to those chosen a priori. To better understand the sources of larvae that are removed by the intake and the percentage of source contributions from different locations, we conducted a backward tracking scenario during a moderate (mean) flow condition.

The backward particle tracking method was applied to the James River model. Starting from 11 May 2017, six particles were released every 20 min from the intake location and tracked from 5 November to 5 May, and a total of 2886 particles were released. The average flow during the tracking period was 34.53 m^3 s^{-1}, close to the mean discharge rate of 35.7 m^3 s^{-1} over the 50-year time series. The locations of particles were output every half hour. Both the frequency of the presence of larvae that were removed by the intake in one grid cell and the contribution from each grid cell were computed.

3. Results and Discussion

3.1. Impact of the Intake on Hydrodynamics

To evaluate the impact of the intake that has a relatively large water withdrawal rate of 40 mgd on local hydrodynamics, we conducted two model runs, case "Normal", where the intake is not present, and case "Withdrawal", where the intake is present and operating. The withdrawal of freshwater by the intake will likely have a larger impact on hydrodynamics during the low-flow summer period. Therefore, we chose the summer of 2017 as our reference period, when discharge was at about the 10th percentile of the long-term river discharge of the Appomattox River.

We compared the horizontal velocities at the surface and bottom at one location in the intake area (Figures 4a–c and S5). We found significant differences in the horizonal velocities between the two cases. The difference in horizontal velocities at the surface was up to 0.109 m s^{-1}, with a mean of 0.025 m s^{-1} during this period, whereas the surface velocity had a mean of 0.173 m s^{-1} and a maximum of 0.344 m s^{-1} under the "Normal" condition. The time series of elevations between the two cases were also compared at the same location (Figure 4d–f). There is a small decrease in elevation (on the order of 1 mm) when the intake was operating compared with "Normal" conditions, which indicates that the total volume of water does not change as the tide dominates the transport of water into the Appomattox River. Meanwhile, the intake affects bottom horizontal velocities near the intake when operating during low-flow periods, and, at a maximum withdrawal rate of 40 mgd, there is not a significant change in water volume.

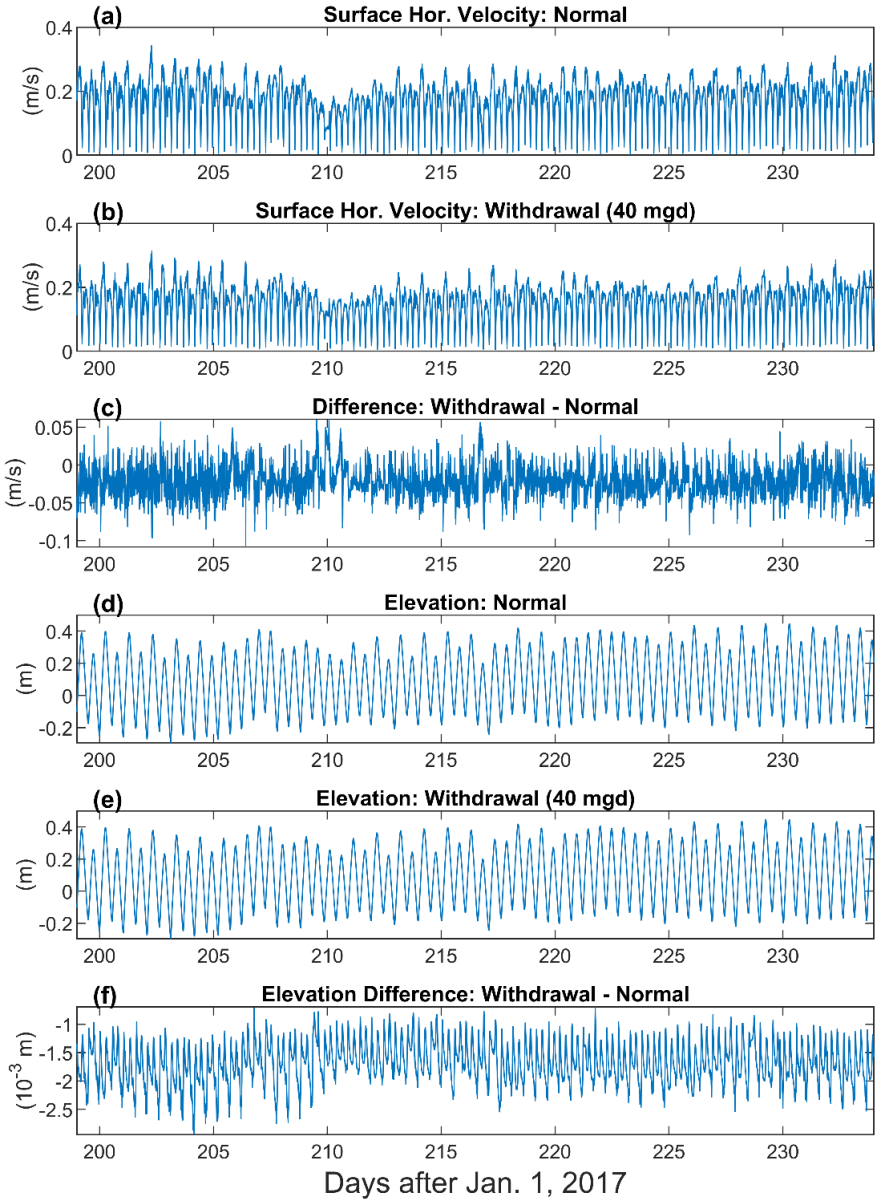

Figure 4. Time series of the speed of surface horizontal velocities (**a**–**c**) and elevation (**d**–**f**) at one location of the intake area under "Normal" (without the intake) and "Withdrawal" (with the intake) conditions and the difference between the two conditions.

3.2. Scenarios for Evaluating the Impacts of Release Methods and Locations

3.2.1. Backward Tracking Scenario

After seven days of backward tracking (5 May to 11 May), the cumulative particle distribution covers the entire Appomattox River and a portion of the James River (Figure S6). Ichthyoplankton originating from these areas are the only particles that may be impacted by the intake during the seven-day period.

Frequency

Particles originating in the Appomattox River had a relatively higher frequency of being removed by the intake compared with those that originated in the James River (Figure 5a). The particles located upstream of the intake generally had a higher frequency than the particles located downstream of the intake. We found that the along-estuary gradients of the frequency were less than the cross-sectional gradients. In the cross-sectional direction, the deep channel shows a higher frequency than the shoals. The particles in the channel can be transported downstream at a higher rate than those at the shoals and, therefore, have a higher chance to be removed by the intake. This is the opposite of the flushing effect, which usually shows stronger flushing by tidal currents in the channels than the shoals and less time for particles to be removed by the intake.

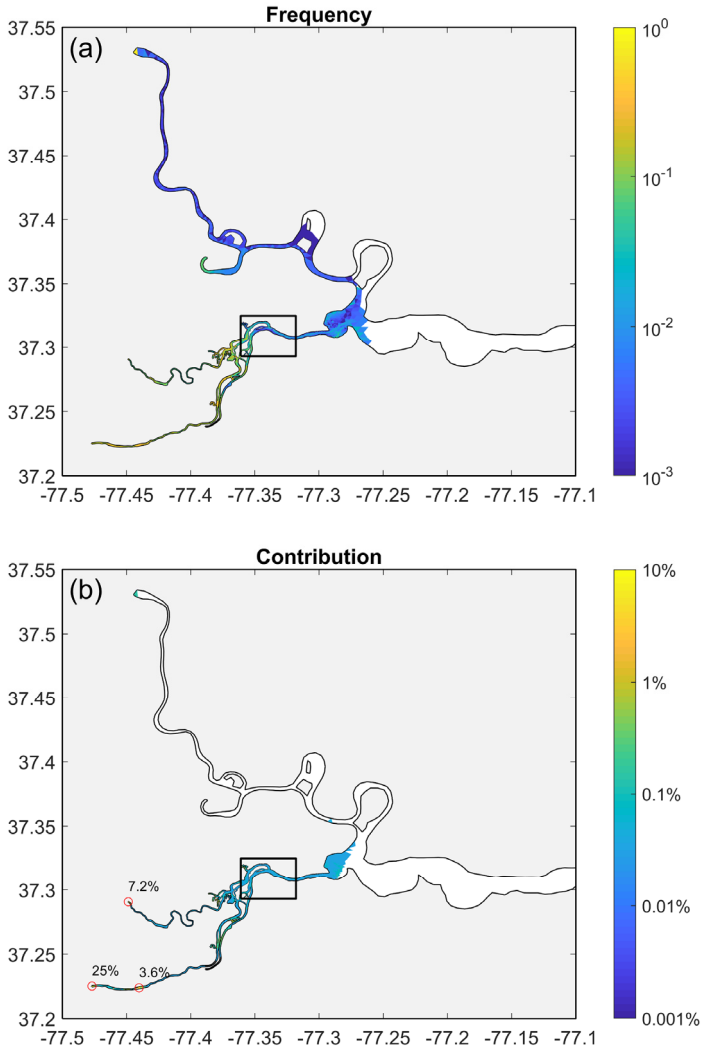

Figure 5. Computed frequency (**a**) and contribution (**b**) of particles released from each location to the particles that encounter the intake during the backward tracking period. The red circles mark the locations with the three highest contributions (=25%, 7.2%, and 3.6%). Note that the location with the

highest contribution marked by the red circle (in (**b**)) is the location where the freshwater discharge enters the Appomattox River in the model.

Contribution

The results from the backward tracking model under moderate flow conditions show that the highest contribution was about 25% at the location where the freshwater discharge enters the Appomattox River in the model domain (Figure 5b). Another branch of the Appomattox River contributed 7.2% of the particles. Because this analysis was based on the distribution of particles on 5 May 2017 in the study area, this suggests that about 25% percent of the particles that were removed by the intake during the seven-day tracking period originally came from the upstream area of the Appomattox River. Additionally, the contribution of particles from the James River was low or equal to zero, indicating that few particles are removed by the intake under moderate flow from the James River. Considering other locations within the Appomattox River, the maximum contribution was about 3.6% at a location near the head. This indicates that particles appearing at this location contributed to about 3.6% of the total particles that were removed by the intake from the entire system during the simulation period. Note that not all the particles that appear in a particular grid cell will ultimately be removed by the intake. To compute the fraction of particles from a grid cell that are removed by the intake, the forward particle tracking model is needed.

3.2.2. Forward Tracking Scenarios

Under scenario 1, particles in the Appomattox River move downstream within the first few hours (Figure 6a,b), and then, after a change from ebb to flood tide, particles are transported back upstream by the incoming flood tide (Figure 6c). As the tides change and particles are dispersed, a few (n = 37) are removed by the intake (i.e., entrained, impinged, or damaged through contact; Figure 6d). Ten days after release, most particles have been transported into the James River and the number of particles that are removed by the intake reaches the maximum (n = 57; Figure 6e,f). Under scenario 2, particles are transported from the release location to the vicinity of the intake within one day (Figure S7a,b). Tidal processes transport the particles back and forth across the location of the intake, and the number of particles that are removed by the intake increases from eight particles on 11 April to 80 particles on 12 April (Figure S7c, flood tide; and Figure S7d, ebb tide). As time continues, the number of particles that are removed by the intake increases to 171 on 16 April, although most have been transported out of the Appomattox River and into the James River (Figure S7e). Eight days after the initial release, the number of particles that are removed by the intake reaches 180 (Figure S7f). Under scenarios 3, 4, and 5, where the release locations occurred downstream of the intake, the only way for particles to reach the intake is through tidal transport, and the overall number of particles that are removed by the intake was low (n = 3) or zero (Figures S8–S10, respectively). For one-time release scenarios, particles are removed by the intake within the first few days after initial release (Figure 7).

Under continuous release scenario 6, where particles are released upstream of the intake in the Appomattox River, particles are removed by the intake over a 25-day period (Figure 7). A total of 74 particles are eventually removed by the intake (Figure S11). By contrast, under scenario 7, where particles are continuously released in the James River upstream of the mouth of the Appomattox River, all the particles are transported downstream and none are removed by the intake (Figure S12).

Under moderate flow conditions, scenario 2 (one-time release upstream of the intake) resulted in the highest number of particles (n = 186) and the highest percent of particles (1.8%) that were removed by the intake (Table 3). The second most impactful scenario, scenario 6 (continuous releases at the head of the Appomattox River), resulted in the removal of 0.74% of the particles. Under scenario 1 (one-time release near the intake), 0.55% of the particles were removed by the intake. Only one other scenario (scenario 3) resulted in a loss of particles, with the remaining three scenarios showing no loss (Table 3).

These results show that particles released from locations downstream of the intake in the Appomattox River or in the James River are much less likely to be removed by the intake under mean flow conditions compared with release locations upstream or near the intake in the Appomattox River.

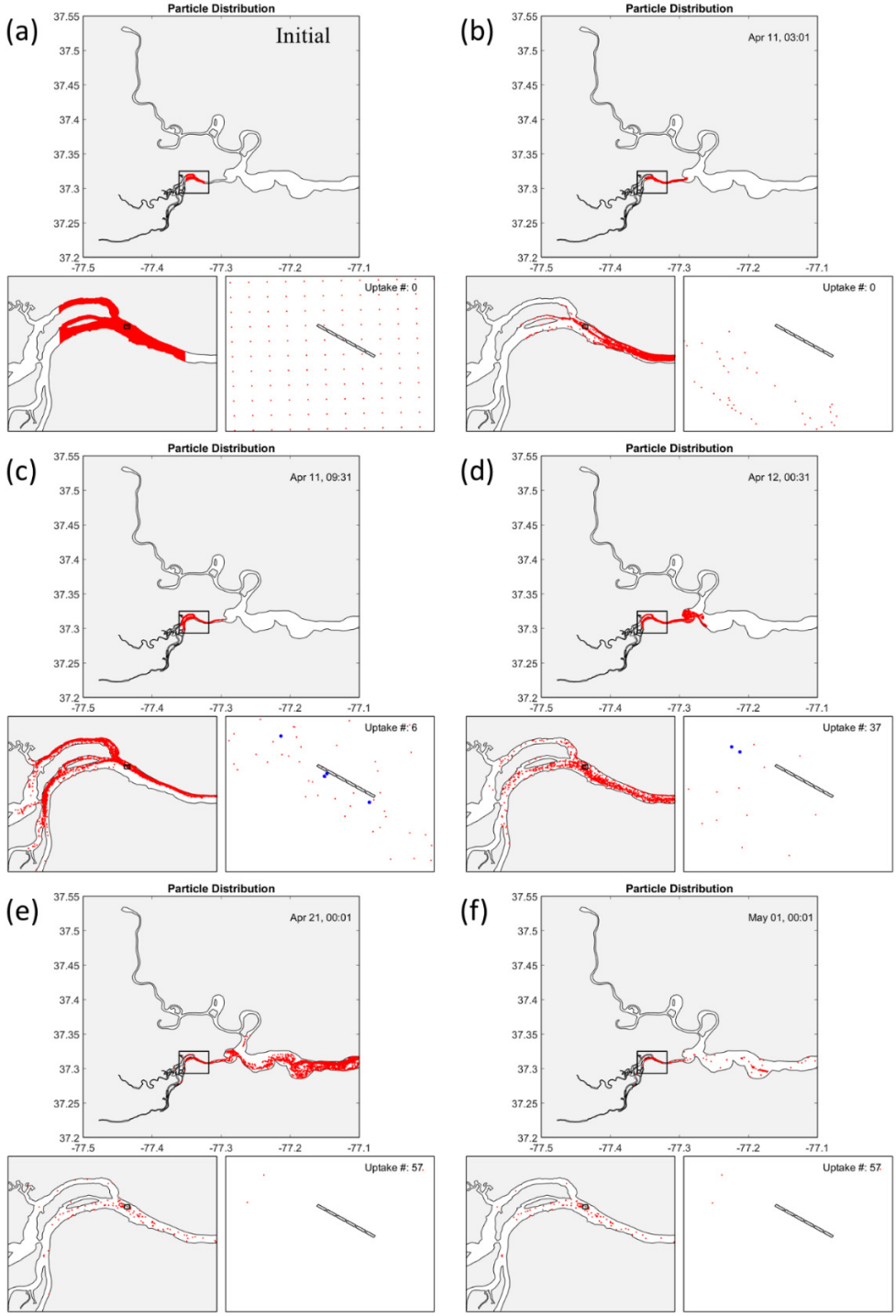

Figure 6. Distribution of particles (red dots) in scenario 1. (**a**) Initial distribution at 11 April 2017. (**b**) After 3 h. (**c**) After 9.5 h. (**d**) After 1 day and a half hour. (**e**) After 10 days. (**f**) After 20 days. Blue dots denote those particles that are eventually removed by the intake.

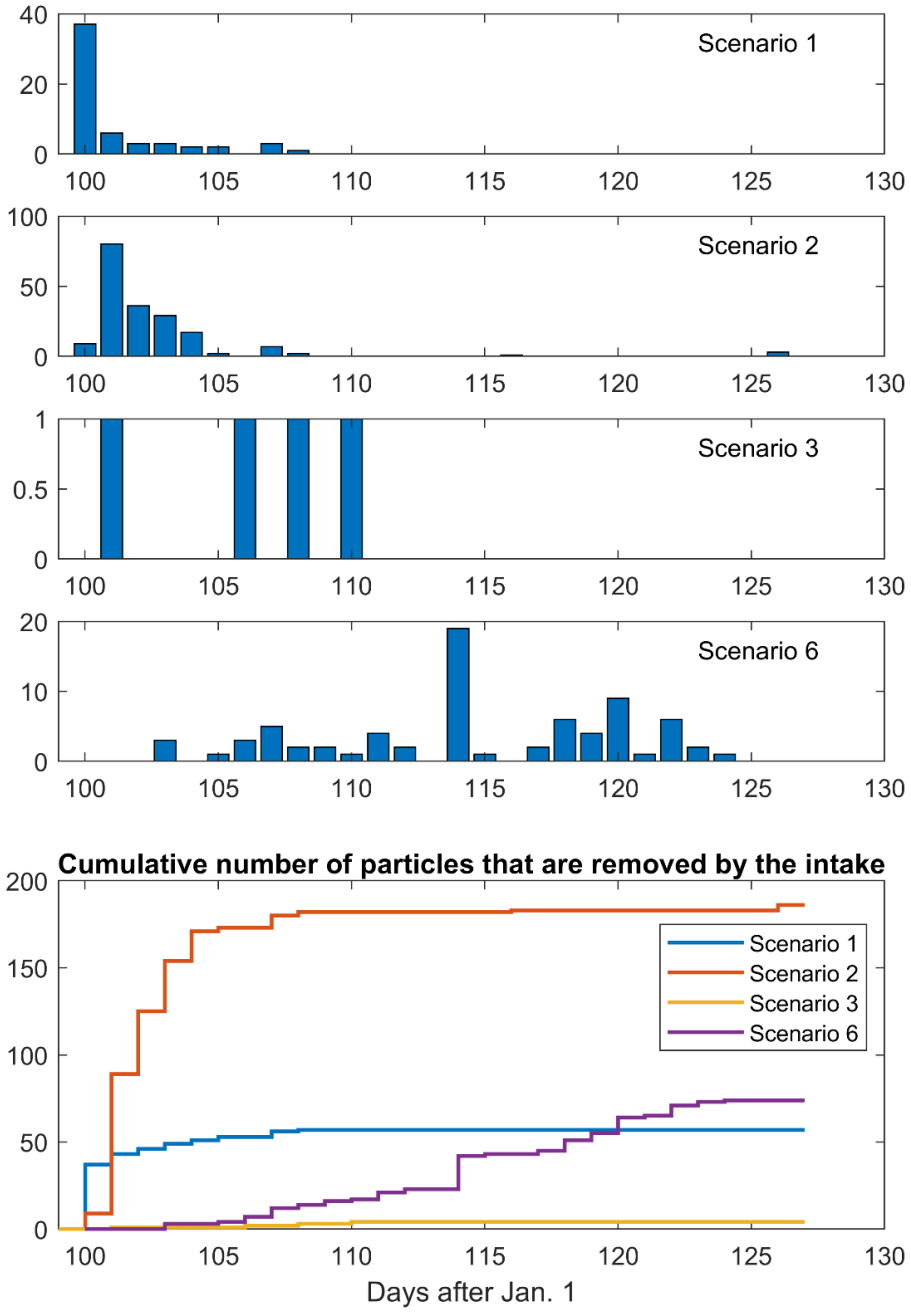

Figure 7. Daily statistics of the number of particles that are removed by the intake for scenarios 1, 2, 3, and 6.

Table 3. The statistics of forward particle tracking scenarios 1–7. Kruskal–Wallis test shows that the difference between the scenarios is significant (p-value < 10^{-6}).

Scenario	Total Number of Particles Released	Number of Particles that Are Removed by the Intake	Percent of Particles that Are Removed by the Intake	Maximum Daily Percent
1	10,385	57	0.55%	0.36%
2	10,349	186	1.80%	0.77%
3	10,179	4	0.04%	0.01%
4	10,801	0	0	0
5	11,466	0	0	0
6	10,000	74	0.74%	0.19%
7	10,000	0	0	0

3.2.3. Summary of Passive Particle Simulations

The results from the forward and backward tracking models show that particles released from locations upstream of the intake are more likely to be removed than those released from downstream locations. River discharge from the Appomattox and James rivers quickly transports particles downstream and away from the intake, whereas tidal processes disperse particles upstream and downstream, and river discharge likely dominates the particle transport process when flow is moderate. Thus, only a small portion of released particles are transported upstream after their initial release and all particles are eventually transported downstream.

3.3. Scenarios That Examine Potential Impacts of River Discharge

Under one-time release scenarios, we compared the results of previous scenarios with the same release location but under different flow conditions (scenarios 1, 8, and 9; scenarios 2, 10, and 11). We found that a lower discharge rate led to higher total removal of particles by the intake (Table 4 and Figure S13). This was expected because a lower discharge rate results in weaker downstream transport of particles and longer retention, thus increasing the probability of particles being removed. Under scenario 9 (low flow), the highest percent of particles removed was 5.44% (Table 4). Under high flow conditions, the particles were advected outside of the study area more quickly, and neither scenario resulted in any loss.

Under continuous release scenarios 12 and 13, a greater proportion of total particles are released with the highest discharge rate and the particle number around the intake increases; however, this does not increase the percent of particles that are removed by the intake because the higher discharge rate leads to stronger advection and more particles are advected outside the study area. Scenario 13 (continuous release upstream of the Appomattox River under low flow conditions) resulted in the highest percent (3.48%) of particles that were removed. Nevertheless, the total percent removed may not only depend on the mean discharge over the tracking period but may also depend on the location of the intake screens or the pattern of flow variability during the study period.

Table 4. Summary of the forward particle tracking scenarios 8–13, considering the impact of flow conditions. Kruskal–Wallis test shows that the difference between the scenarios is significant (p-value < 10^{-6}).

Scenario	Total Number of Particles Released	Number of Particles that are Removed by the Intake	Percent of Particles that are Removed by the Intake	Maximum Daily Percent
8	10,385	0	0	0
9	10,385	565	5.44%	0.70%
10	10,349	0	0	0
11	10,349	403	3.89%	0.39%
12	10,001	20	0.20%	0.03%
13	9999	348	3.48%	0.41%

3.4. Scenarios Investigating Active Particles

We conducted 21 scenarios to investigate active particles with seven different vertical velocities that represent sinking eggs and larvae with swimming behaviors. Active particles alter their position in the water column, and this interacts with the hydrodynamic field and changes the potential dispersal pattern relative to passive particles.

Active particles released near the intake (scenarios 14–20) resulted in a higher removal rate compared with the release of particles upstream of the intake (scenarios 21–27; Table 5). The largest removal rate was 4.30% (scenario 18), with a settling velocity of -0.001 cm s^{-1}, which was slightly lower than that observed for passive particles under scenario 9 (5.44%).

Particles with relatively fast settling velocities (-1, -0.3, and -0.1 cm s^{-1}) experienced higher removal rates during the first two days compared with scenarios with relatively slow settling velocities (-0.01 and -0.001 cm s^{-1}; Figure 8). Fast settling velocities result

in fewer particles in the water column that are available to the intake, so they are only vulnerable for the first few tidal cycles. Conversely, slower settling velocities increase the chance that particles encounter the intake because more particles remain in the water column, increasing the possibility of removal in subsequent tidal cycles. In the extreme case, the lowest settling velocity described by scenario 9 (passive particle under low flow) shows that the highest daily removal rate was not until the third day (Figure S13).

Seven continuous release scenarios with active particles were investigated, and those with upward velocities or relatively fast downward settling velocities (scenarios 28–30 and 33–34) showed no loss due to the intake, indicating the low chance for demersal eggs or larvae to encounter the intake if they are spawned at the upstream locations that are beyond the model domain. The greatest impact observed for active particles under continuous release scenarios was under scenario 32, with a relatively slow settling velocity of -0.001 cm s^{-1} and a removal rate of 1.61% (Table 5).

It was interesting to find that the scenarios with particles released upstream of the intake (either one-time or continuous releases) resulted in lower removal rates compared with releases near the intake. The low removal rate for active particles suggests that downward settling particles will settle to the bottom and will end their journey before reaching the intake. Active particles with upward swimming velocities will travel a much longer distance than particles that settle, but they remain near the surface and have little chance of removal by the intake located near the riverbed.

Table 5. The statistics of forward particle tracking scenarios 14–34. The vertical velocity of the particle can be either upward (+) or downward (−).

Scenario	Vertical Velocity (cm s^{-1})	Representative	Total Number of Particles Released	Number of Particles that Are Removed by the Intake	Percent of Particles that Are Removed by the Intake	Maximum Daily Percent
14	−1	Demersal egg	10,385	421	4.05%	2.57%
15	−0.3	Demersal egg	10,385	240	2.31%	1.26%
16	−0.1	Demersal egg	10,385	294	2.83%	1.21%
17	−0.01	Demersal egg	10,385	145	1.40%	0.58%
18	−0.001	Demersal egg	10,385	447	4.30%	0.74%
19	1	larvae	10,385	0	0	0
20	10	larvae	10,385	0	0	0
21	−1	Demersal egg	10,349	0	0	0
22	−0.3	Demersal egg	10,349	0	0	0
23	−0.1	Demersal egg	10,349	0	0	0
24	−0.01	Demersal egg	10,349	1	0.01%	0.01%
25	−0.001	Demersal egg	10,349	153	1.48%	0.14%
26	1	larvae	10,349	0	0	0
27	10	larvae	10,349	0	0	0
28	−1	Demersal egg	9999	0	0	0
29	−0.3	Demersal egg	9999	0	0	0
30	−0.1	Demersal egg	9999	0	0	0
31	−0.01	Demersal egg	9999	1	0.01%	0.01%
32	−0.001	Demersal egg	9999	161	1.61%	0.25%
33	1	larvae	9999	0	0	0
34	10	larvae	9999	0	0	0

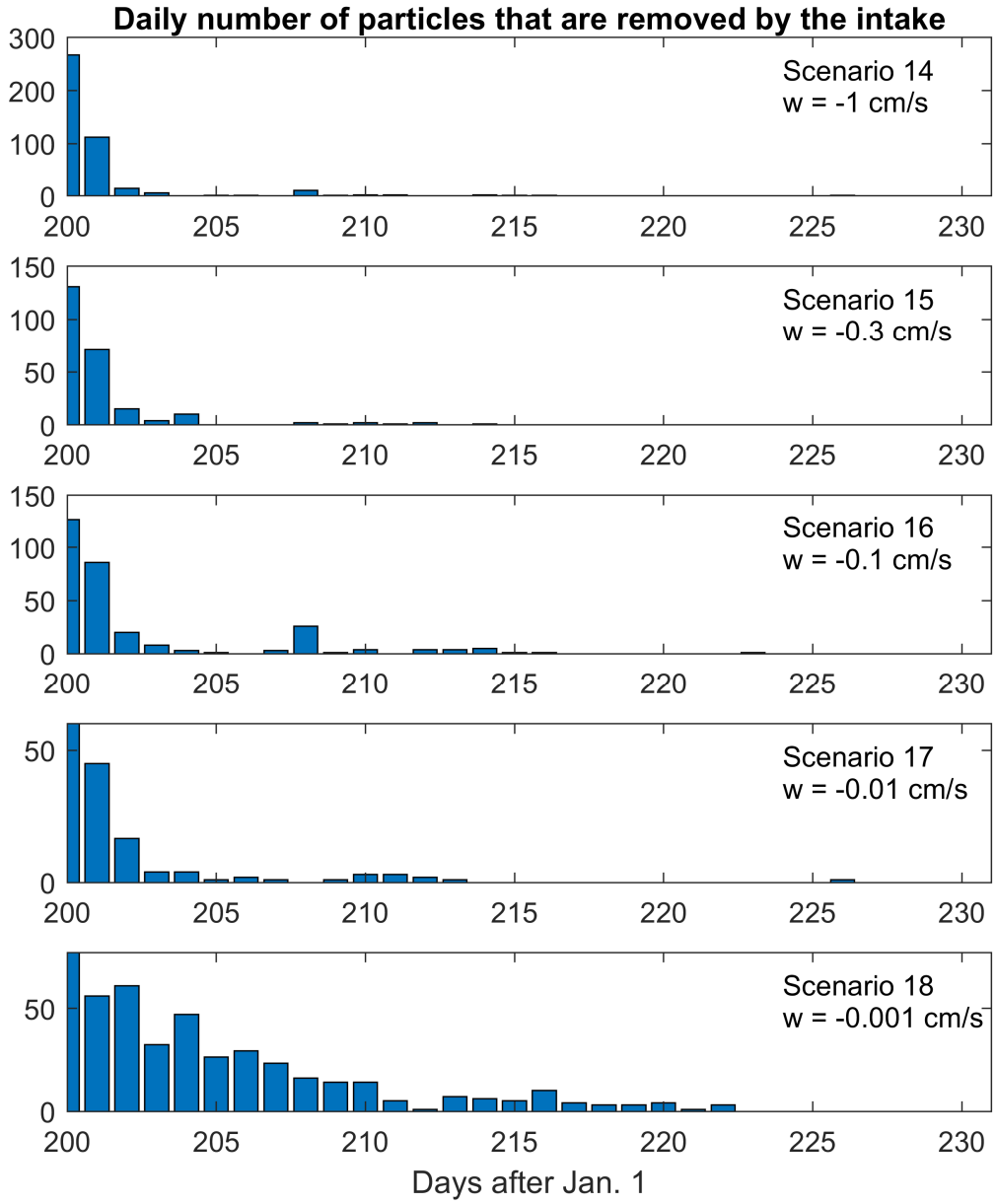

Figure 8. Daily statistics of the number of particles that are removed by the intake for scenarios 14–18, where the release location is around the intake.

3.5. Impact of the Intake on Ichthyoplankton Survival

One main purpose of the present modeling effort was to examine potential impacts of the water intake on ichthyoplankton survival. In this study, the results of 34 different modeling scenarios show that the total percent of particles removed due to the intake ranged from 0 to 4–5%, and the maximum daily removal rate ranged from 0 to 2–3% per day (Figure 9). Because the flow rate near the intake causes a minor change in velocity away from the intake, only particles that are close to the intake will be removed. This suggests that, even under the conservative assumption that impingement and entrainment cause 100% mortality of the ichthyoplankton that encounter the intake, the conditional mortality rate caused by the intake is estimated to be below 4–5%. If there is potential for survival of entrained ichthyoplankton for some species, as suggested by some experimental studies [41], then the conditional mortality rate would be even lower. It is known that natural mortality is typically high for ichthyoplankton, and most estimates of the mortality are approximately 20% per day [42,43]. For example, among the three representative fish species in the region, larvae of striped bass have the lowest daily mortality of 10.4–32.9%, while

larvae of blueback herring and inland silverside have daily mortality rates of 88–99%; other fish species also have natural daily mortality rates much greater than 2–3% [15,17,44–50]. Thus, mortality due to the intake is orders of magnitude less than natural mortality. From this modeling study, the intake operation with a flow rate of 40 mgd has a low impact on ichthyoplankton survival in this area. While there is increased mortality due to the intake, the increase is unlikely to cause serious harm to fish eggs and larvae.

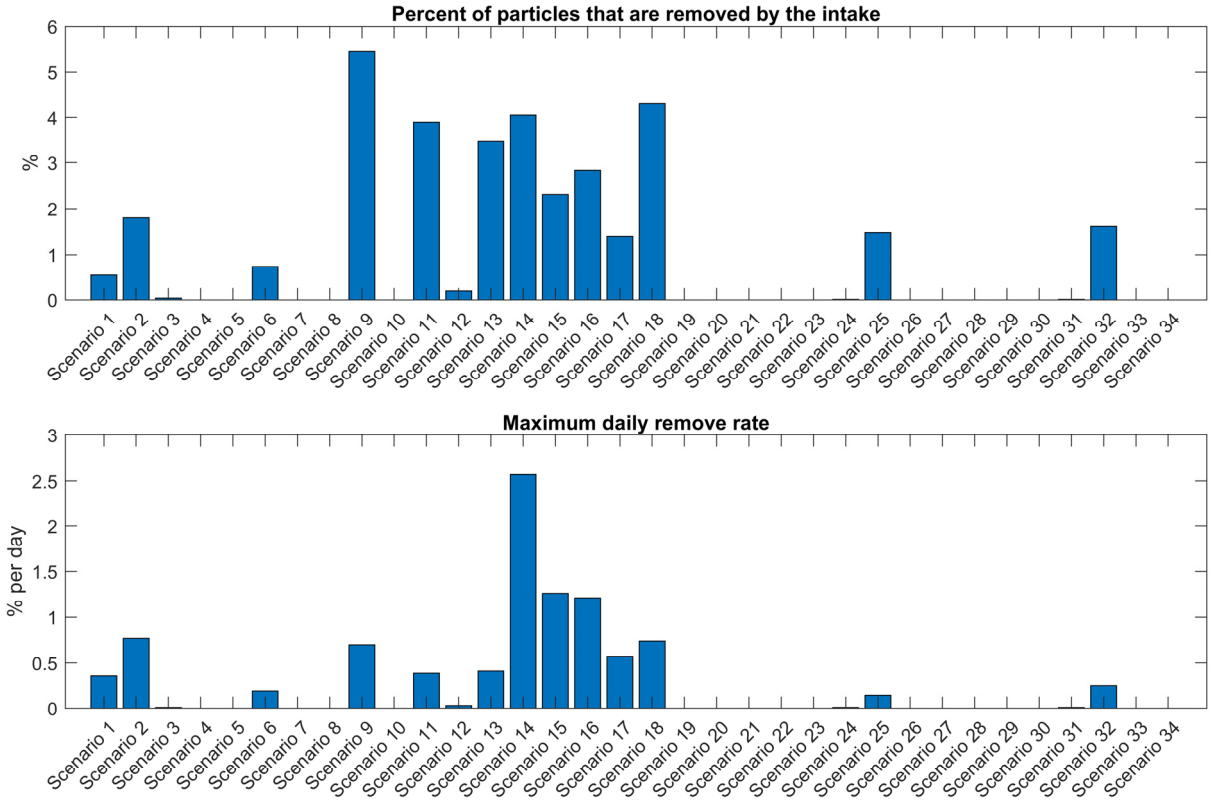

Figure 9. A summary of all the forward-tracking scenarios showing the total number of particles removed by the intake (i.e., percent of particles that are removed by the intake) and the maximum daily removal rate.

4. Conclusions

We investigated the potential impacts of a proposed municipal water intake on the survival of ichthyoplankton in a tidal freshwater estuary. We used an unstructured grid model with fine resolution in the vicinity of the intake to simulate river hydrodynamics and a particle tracking model to simulate the transport of ichthyoplankton (passive and active particles). The model results show that the intake, with a withdrawal rate of 40 mgd, can alter the velocity of the tidal flow near the intake but does not have significant impacts on the hydrodynamics in the Appomattox River.

Forward and backward particle tracking approaches were used to investigate the potential impacts of the intake. Two variables, "frequency" and "contribution", were introduced and computed in the backward tracking scenario to identify the major sources of ichthyoplankton that were removed by the intake. Ichthyoplankton that are found in the channel have a greater probability of being removed by the intake than those found along the shoals due to the flushing effect created by faster currents in the channel. Additionally, ichthyoplankton that originate upstream of the intake are removed to a greater extent than those originating downstream of the intake. The model results also show an increase in the percent of ichthyoplankton that are removed during dry years or seasons under low flow conditions. Since spawning seasons of other species will likely encompass low flow

periods, our results suggest impacts could be more important for those species that spawn during dry summer months.

The pathways of active particles were different from passive particles, indicating that the vertical velocity of ichthyoplankton can alter the transport and distribution of eggs and larvae and, hence, the removal rate due to the intake. For example, particles that represent demersal eggs with negative vertical velocities had a variety of outcomes, with only the slowest sinking rates resulting in removal by the intake if they were released upstream. Additionally, for particles that represent larvae with upward swimming velocities, the current location and design of the intake likely have limited impacts because the screens were located in the lower half of the water column and larvae at the surface avoided the intake. Thus, larval fish behavior can alter impacts from water intakes, with those impacts determined by swimming speeds and location relative to the intake. Furthermore, other behaviors not studied here could alter impacts of water intakes, such as daily migration between surface waters at night and bottom waters during day. These different migration patterns are more complex and require additional modeling efforts.

The total removal (percent) of particles and the maximum daily removal rate in all the model scenarios was below 5% and 3%, respectively, which is an order of magnitude lower than natural mortality rates of ichthyoplankton. This indicates that the current design of the intake has comparatively low impacts on the ichthyoplankton in this estuary, although the losses are real and a direct result of the intake. The numerical modeling approach used here simulates ichthyoplankton dispersal and changes in mortality caused by the intake under a variety of river flow conditions (e.g., high, average, and low flows), which provides scientific-based assessment of potential impacts that would otherwise not be possible.

Supplementary Materials: The following supporting information can be downloaded at: https://www.mdpi.com/article/10.3390/jmse10091299/s1, Table S1: Comparison between current scenarios and 10-fold scenarios; Figure S1: Initial distribution of 10,385 particles in Scenario 1; Figures S2–S4: Number of particles release under Scenarios 6, 12, and 13, respectively; Figure S5: Time series of bottom horizontal velocities at one location of the intake area under "Normal" (without the intake) and "Withdrawal" (with the intake) states, and the difference between the two states; Figure S6: Cumulative distribution of particles originally released from the location of the intake in the back-tracking scenario; Figures S7–S12: Distribution of particles in Scenarios 2–7, respectively; Figure S13: Daily statistics of the number of particles that are removed by the intake for Scenarios 9, 11, 12, and 13, respectively.

Author Contributions: Conceptualization, J.S. and Q.Q.; methodology, Q.Q. and J.S.; software, Q.Q., X.C. and J.X.; validation, Q.Q., J.S. and X.C.; formal analysis, Q.Q.; investigation, Q.Q. and T.D.T.; resources, T.D.T. and J.S.; data curation, Q.Q. and X.C.; writing—original draft preparation, Q.Q.; writing—review & editing, J.S., T.D.T. and J.X.; visualization, Q.Q.; supervision, J.S. and T.D.T.; funding acquisition, J.S. All authors have read and agreed to the published version of the manuscript.

Funding: The funding for this study was provided by Chesterfield County, Virginia (number 778870).

Institutional Review Board Statement: Not applicable.

Informed Consent Statement: Not applicable.

Data Availability Statement: Not applicable.

Acknowledgments: We thank Lyle M. Varnell for his proofreading and constructive suggestions. We also thank Paul E. Peterson of ARCADIS U.S., Inc., and the scientists of Chesterfield County for proving many suggestions during the course of the study. The authors acknowledge William & Mary Research Computing for providing computational resources that have contributed to the results reported within this paper (https://www.wm.edu/it/rc, accessed on 12 September 2022). This paper is Contribution No. 4119 of the Virginia Institute of Marine Science, William & Mary.

Conflicts of Interest: The authors declare no conflict of interest.

References

1. EPA (United States Environmental Protection Agency). National pollutant discharge elimination system—Final regulations to establish requirements for cooling water intake structures at existing facilities and amend requirements at phase I facilities. *Fed. Regist.* **2014**, *79*, 48299–48439.
2. Hogan, T.W. Impingement and entrainment at SWRO desalination facility intakes. In *Intakes and Outfalls for Seawater Reverse-osmosis Desalination Facilities: Innovations and Environmental Impacts*; Missimer, T.M., Jones, B., Maliva, R.G., Eds.; Springer International Publishing: Cham, Switzerland, 2015; pp. 57–78.
3. Missimer, T.M.; Maliva, R.G. Environmental Issues in Seawater Reverse Osmosis Desalination: Intakes and Outfalls. *Desalination* **2018**, *434*, 198–215. [CrossRef]
4. Varnell, L.M.; Evans, D.A.; Bilkovic, D.M.; Olney, J.E. Estuarine Surface Water Allocation: A Case Study on the Interactive Role of Science in Support of Management. *Environ. Sci. Policy* **2008**, *11*, 602–612. [CrossRef]
5. Barnthouse, L.W. Impacts of Entrainment and Impingement on Fish Populations: A Review of the Scientific Evidence. *Environ. Sci. Policy* **2013**, *31*, 149–156. [CrossRef]
6. Barnthouse, L.W.; Boreman, J.; Christensen, S.W.; Goodyear, C.P.; van Winkle, W.; Vaughan, D.S. Population Biology in the Courtroom: The Hudson River Controversy. *BioScience* **1984**, *34*, 14–19. [CrossRef]
7. Grimaldo, L.F.; Sommer, T.; van Ark, N.; Jones, G.; Holland, E.; Moyle, P.B.; Herbold, B.; Smith, P. Factors Affecting Fish Entrainment into Massive Water Diversions in a Tidal Freshwater Estuary: Can Fish Losses Be Managed? *N. Am. J. Fish. Manag.* **2009**, *29*, 1253–1270. [CrossRef]
8. EPRI (Electric Power Research Institute). *Laboratory Evaluation of Wedgewire Screens for Protecting Early Life Stages of Fish at Cooling Water Intakes*; EPRI Report No. 1005339; EPRI (Electric Power Research Institute): Palo Alto, CA, USA, 2003.
9. Blumberg, A.F.; Dunning, D.J.; Li, H.; Heimbuch, D.; Geyer, W.R. Use of a Particle-Tracking Model for Predicting Entrainment at Power Plants on the Hudson River. *Estuaries* **2004**, *27*, 515–526. [CrossRef]
10. White, J.W.; Nickols, K.J.; Clarke, L.; Largier, J.L. Larval Entrainment in Cooling Water Intakes: Spatially Explicit Models Reveal Effects on Benthic Metapopulations and Shortcomings of Traditional Assessments. *Can. J. Fish. Aquat. Sci.* **2010**, *67*, 2014–2031. [CrossRef]
11. Heimbuch, D.G.; Dunning, D.J.; Ross, Q.E.; Blumberg, A.F. Assessing Potential Effects of Entrainment and Impingement on Fish Stocks of the New York–New Jersey Harbor Estuary and Long Island Sound. *Trans. Am. Fish. Soc.* **2007**, *136*, 492–508. [CrossRef]
12. Norcross, B.L.; Shaw, R.F. Oceanic and Estuarine Transport of Fish Eggs and Larvae: A Review. *Trans. Am. Fish. Soc.* **1984**, *113*, 153–165. [CrossRef]
13. Qin, Q.; Shen, J. The Contribution of Local and Transport Processes to Phytoplankton Biomass Variability over Different Timescales in the Upper James River, Virginia. *Estuar. Coast. Shelf Sci.* **2017**, *196*, 123–133. [CrossRef]
14. Buchanan, J.R.; Fabrizio, M.C.; Tuckey, T.D. *Estimation of Juvenile Striped Bass Relative Abundance in the Virginia Portion of Chesapeake Bay*; Final Report to the Virginia Marine Resources Commssion, F87R32; College of William & Mary: Gloucester Point, VA, USA, 2021. [CrossRef]
15. Walsh, H.J.; Settle, L.R.; Peters, D.S. Early Life History of Blueback Herring and Alewife in the Lower Roanoke River, North Carolina. *Trans. Am. Fish. Soc.* **2005**, *134*, 910–926. [CrossRef]
16. Hubbs, C. Life History Dynamics of *Menidia beryllina* from Lake Texoma. *Am. Midl. Nat.* **1982**, *107*, 1–12. [CrossRef]
17. Froese, R.; Pauly, D. (Eds.) World Wide Web Electronic Publication. FishBase. 2019. Available online: www.fishbase.org (accessed on 1 December 2019).
18. Mansueti, R.J. *Eggs, Larvae and Young of the Striped Bass, Roccus Saxatilis*; Maryland Department of Research and Education, Contribution No. 112; Chesapeake Biological Laboratory: Solomons, MD, USA, 1958.
19. Grant, G.C.; Olney, J.E. *Assessment of Lrval Striped Bass, Morone saxatilis (Walbaum), Stocks in Maryland and Virginia Waters. Part II. Assessment of Spawning Activity in Major Virginia Rivers. Segment 2. Distribution and Abundance of Striped Bass Eggs and Larvae in the James and Chickahominy Rivers, Virginia, during Spring 1981: Draft Final Report*; Virginia Institute of Marine Science, William & Mary: Gloucester Point, VA, USA, 1982. [CrossRef]
20. Ye, F.; Zhang, Y.J.; Wang, H.V.; Friedrichs, M.A.M.; Irby, I.D.; Alteljevich, E.; Valle-Levinson, A.; Wang, Z.; Huang, H.; Shen, J.; et al. A 3D Unstructured-Grid Model for Chesapeake Bay: Importance of Bathymetry. *Ocean Model* **2018**, *127*, 16–39. [CrossRef]
21. Cai, X.; Zhang, Y.J.; Shen, J.; Wang, H.; Wang, Z.; Qin, Q.; Ye, F. A Numerical Study of Hypoxia in Chesapeake Bay Using an Unstructured Grid Model: Validation and Sensitivity to Bathymetry Representation. *J. Am. Water Resour. Assoc.* **2020**. [CrossRef]
22. Cai, X.; Shen, J.; Zhang, Y.J.; Qin, Q.; Wang, Z.; Wang, H. Impacts of Sea-Level Rise on Hypoxia and Phytoplankton Production in Chesapeake Bay: Model Prediction and Assessment. *J. Am. Water Resour. Assoc.* **2021**. [CrossRef]
23. Zhang, Y.J.; Ye, F.; Stanev, E.V.; Grashorn, S. Seamless Cross-Scale Modeling with SCHISM. *Ocean Model* **2016**, *102*, 64–81. [CrossRef]
24. Zhang, Y.J.; Ateljevich, E.; Yu, H.C.; Wu, C.H.; Yu, J.C.S. A New Vertical Coordinate System for a 3D Unstructured-Grid Model. *Ocean Model* **2015**, *85*, 16–31. [CrossRef]
25. Gallego, A.; North, E.W.; Petitgas, P. Introduction: Status and Future of Modelling Physical-Biological Interactions during the Early Life of Fishes. *Mar. Ecol. Prog. Ser.* **2007**, *347*, 121–126. [CrossRef]

26. Torri, M.; Corrado, R.; Falcini, F.; Cuttitta, A.; Palatella, L.; Lacorata, G.; Patti, B.; Arculeo, M.; Mifsud, R.; Mazzola, S.; et al. Planktonic Stages of Small Pelagic Fishes (*Sardinella aurita* and *Engraulis encrasicolus*) in the Central Mediterranean Sea: The Key Role of Physical Forcings and Implications for Fisheries Management. *Prog. Oceanogr.* **2018**, *162*, 25–39. [CrossRef]
27. Chiu, C.M.; Huang, C.J.; Wu, L.C.; Zhang, Y.J.; Chuang, L.Z.H.; Fan, Y.; Yu, H.C. Forecasting of Oil-Spill Trajectories by Using SCHISM and X-Band Radar. *Mar. Pollut. Bull.* **2018**, *137*, 566–581. [CrossRef] [PubMed]
28. Du, J.; Park, K.; Yu, X.; Zhang, Y.J.; Ye, F. Massive Pollutants Released to Galveston Bay during Hurricane Harvey: Understanding Their Retention and Pathway Using Lagrangian Numerical Simulations. *Sci. Total Environ.* **2020**, *704*, 135364. [CrossRef]
29. Xiong, J.; Shen, J.; Qin, Q.; Tomlinson, M.C.; Zhang, Y.J.; Cai, X.; Ye, F.; Cui, F.; Mulholland, M.R. Biophysical interactions control the progression of harmful algal blooms in Chesapeake Bay: A novel Lagrangian particle tracking model with mixotrophic growth and vertical migration. *Limnol. Oceanogr. Lett.* **2022**. Submitt.
30. Dey, S.; Ali, S.Z.; Padhi, E. Terminal Fall Velocity: The Legacy of Stokes from the Perspective of Fluvial Hydraulics. *Proc. R. Soc. A Math. Phys. Eng. Sci.* **2019**, *475*, 20190277. [CrossRef] [PubMed]
31. Sundby, S.; Kristiansen, T. The Principles of Buoyancy in Marine Fish Eggs and Their Vertical Distributions across the World Oceans. *PLoS ONE* **2015**, *10*, e0138821. [CrossRef]
32. Bergey, L.L.; Rulifson, R.A.; Gallagher, M.L.; Overton, A.S. Variability of Atlantic Coast Striped Bass Egg Characteristics. *N. Am. J. Fish. Manag.* **2003**, *23*, 558–572. [CrossRef]
33. Kowalik, D.M.; Eakin, W.W. N-Mixture Modeling of River Herring Egg Abundance and Distribution in the Tributaries of the Hudson River. *Mar. Coast. Fish.* **2019**, *11*, 48–61. [CrossRef]
34. Sundby, S. A One-Dimensional Model for the Vertical Distribution of Pelagic Fish Eggs in the Mixed Layer. *Deep. Sea Res. Part A Oceanogr. Res. Pap.* **1983**, *30*, 645–661. [CrossRef]
35. Ferguson, R.I.; Church, M. A Simple Universal Equation for Grain Settling Velocity. *J. Sediment. Res.* **2004**, *74*, 645–661. [CrossRef]
36. Brandt, L.; Coletti, F. Particle-Laden Turbulence: Progress and Perspectives. *Annu. Rev. Fluid Mech.* **2021**, *54*, 159–189. [CrossRef]
37. Shen, J.; Qin, Q. *James River Water Quality Model Refinement and Scenario Simulations*; Special Reports in Applied Marine Science and Ocean Engineering (SRAMSOE) No. 474; Virginia Institute of Marine Science, William & Mary: Gloucester Point, VA, USA, 2019. [CrossRef]
38. Downie, A.T.; Illing, B.; Faria, A.M.; Rummer, J.L. Swimming Performance of Marine Fish Larvae: Review of a Universal Trait under Ecological and Environmental Pressure. *Rev. Fish Biol. Fish.* **2020**, *30*, 93–108. [CrossRef]
39. Peterson, R.H.; Harmon, P. Swimming Ability of Pre-Feeding Striped Bass Larvae. *Aquac. Int.* **2001**, *9*, 361–366. [CrossRef]
40. Geyer, W.R.; Signell, R.P. A Reassessment of the Role of Tidal Dispersion in Estuaries and Bays. *Estuaries* **1992**, *15*, 97–108. [CrossRef]
41. EPRI (Electric Power Research Institute). *Review of Entrainment Survival Studies: 1970–2000*; EPRI Report No. 1000757; EPRI (Electric Power Research Institute): Palo Alto, CA, USA, 2000.
42. Metaxas, A.; Saunders, M. Quantifying the "Bio-" Components in Biophysical Models of Larval Transport in Marine Benthic Invertebrates: Advances and Pitfalls. *Biol. Bull.* **2009**, *216*, 257–272. [CrossRef] [PubMed]
43. White, J.W.; Morgan, S.G.; Fisher, J.L. Planktonic Larval Mortality Rates Are Lower than Widely Expected. *Ecology* **2014**, *95*, 3344–3353. [CrossRef]
44. Abraham, B.J. Species Profiles: Life Histories and Environmental Requirements of Coastal Fishes and Invertebrates (Mid-Atlantic): Mummichog and Striped Killifish. In *U.S. Fish and Wildlife Service Biological Report*; U.S. Department of the Interior: Washington, DC, USA, 1985.
45. Jenkins, R.E.; Burkhead, N.M. *Freshwater Fishes of Virginia*; American Fisheries Society: Bethesda, MD, USA, 1993.
46. Kneib, R.T. Growth and Mortality in Successive Cohorts of Fish Larvae within an Estuarine Nursery. *Mar. Ecol. Prog. Ser.* **1993**, *94*, 115–127. [CrossRef]
47. Rutherford, E.S.; Houde, E.D.; Nyman, R.M. Relationship of Larval-Stage Growth and Mortality to Recruitment of Striped Bass, *Morone saxatilis*, in Chesapeake Bay. *Estuaries* **1997**, *20*, 174–198. [CrossRef]
48. Limburg, K.E.; Pace, M.L.; Arend, K.K. Growth, Mortality, and Recruitment of Larval *Morone* spp. in Relation to Food Availability and Temperature in the Hudson River. *Fish. Bull.* **1999**, *97*, 80–91.
49. Phillips, E.C.; Ewert, Y.; Speares, P.A. Fecundity, Age and Growth, and Diet of *Fundulus diaphanus* (Banded Killifish) in Presque Isle Bay, Lake Erie. *Northeast Nat.* **2007**, *14*, 269–278. [CrossRef]
50. Greene, K.E.; Zimmerman, J.L.; Laney, R.W.; Thomas-Blate, J.C. *Atlantic Coast Diadromous Fish Habitat: A Review of Utilization, Threats, Recommendations for Conservation, and Research Needs*; ASMFC Habitat Management Series No. 9; Atlantic States Marine Fisheries Commission: Washington, DC, USA, 2009.